

LA-UR-02-5105

Approved for public release;  
distribution is unlimited.

Title: " ATOMISTIC SIMULATIONS OF THE PLASTICITY  
BEHAVIOR OF POLYCRYSTALLINE METALS"

Author(s): Michael I. Baskes, 154516, MST-8

Submitted to: DIS' 02, Osaka, Japan  
Nov. 26-28, 2002



Los Alamos National Laboratory, an affirmative action/equal opportunity employer, is operated by the University of California for the U.S. Department of Energy under contract W-7405-ENG-36. By acceptance of this article, the publisher recognizes that the U.S. Government retains a nonexclusive, royalty-free license to publish or reproduce the published form of this contribution, or to allow others to do so, for U.S. Government purposes. Los Alamos National Laboratory requests that the publisher identify this article as work performed under the auspices of the U.S. Department of Energy. Los Alamos National Laboratory strongly supports academic freedom and a researcher's right to publish; as an institution, however, the Laboratory does not endorse the viewpoint of a publication or guarantee its technical correctness.

Form 836 (8/00)

# ATOMISTIC SIMULATIONS OF THE PLASTICITY BEHAVIOR OF POLYCRYSTALLINE METALS

M. I. Baskes

Structure Property Relations Group  
Los Alamos National Laboratory  
Los Alamos, NM 87501

## Abstract

Recent advances in computers and atomistic modeling have made the realistic simulation of materials behavior possible. Two decades ago, modeling of materials at the atomic level used simple pair potentials. These potentials did not provide an accurate description of the elastic properties of materials or of the formation of free surfaces, a phenomenon critical in the fracture process. This paper will review the evolution of the Embedded Atom Method (EAM), a modern theory of metallic cohesion that was developed to overcome the limitations of pair potentials. The EAM includes many body effects that are necessary to describe such processes as bond weakening (or strengthening) by impurities.

We examine the effects of deformation on polycrystalline FCC metals. We perform simple shear molecular dynamics simulations using the EAM on nickel samples of ~10000 atoms to study yield and work hardening. It is found that the deformation is always inhomogeneous when a grain boundary or free surface is present. The atomistic simulations reveal that dislocations nucleating at grain boundaries or free surfaces are critical to causing yielding in pristine material as observed in experiment [1, 2].

Detailed investigation shows that the grain boundaries are significantly weaker than the bulk material and yield at a lower stress. Even so, the yield stress of the polycrystalline samples with either low angle and high angle grain boundaries are found to be similar and only slightly lower than the yield stress of single crystals with the same characteristic dimensions. The local yield stress at the boundaries is found to be significantly less than the average yield stress.

## 1. INTRODUCTION

Atomistic calculations have been used for a wide variety of materials. All start from atomic pair potentials or some related modification. Daw and Baskes [3] developed the Embedded Atom Method (EAM), which employs a pair potential augmented by a function of another pair-wise sum. This function, the embedding energy, was first suggested by Friedel [4] and further developed by Stott and Zaremba [5]. Daw et al. [6] summarize many applications of EAM.

Horstemeyer et al. [7-12] have previously used such methods to investigate the plastic behavior of single crystal nickel. In this work we extend this work by using atomistic EAM calculations to study finite deformations of polycrystalline nickel.

## 2. EMBEDDED ATOM METHOD

The EAM[3, 6, 13] is used to calculate the cohesive energy of an ensemble of atoms. This energy  $E$  consists of two terms: an embedding energy  $F$  determined by the local electron density at each atom and a repulsive pair potential  $\phi$ .

$$E = \sum_i F^i \left( \sum_{i \neq j} \rho^i(r^{ij}) \right) + \frac{1}{2} \sum_{ij} \phi^{ij}(r^{ij}), \quad (1)$$

The atomic electron density  $\rho(r)$ , is viewed as the contribution to the electron density at a site due to the neighboring atoms. The embedding energy  $F$  is associated with placing an atom in that electron environment. In the summations  $i$  refers to the atom in question and  $j$  refers to the neighboring atom, and  $r^{ij}$  is the separation distance between atoms  $i$  and  $j$ . In molecular dynamics, the energy is used to determine the forces on each atom. At each atom the dipole force tensor,  $\underline{\beta}$ , is given by

$$\beta_{km}^i = \frac{1}{\Omega^i} \sum_{j(\neq i)}^N f_k^i(r^{ij}) r_m^{ij}, \quad (2)$$

where  $i$  refers to the atom in question and  $j$  refers to the neighboring atom,  $f_k$  is the force vector between atoms,  $r_m$  is a displacement vector between atoms  $i$  and  $j$ ,  $N$  is the number of nearest neighbor atoms, and  $\Omega^i$  is the atomic volume. If stress could be defined at an atom, then  $\underline{\beta}$  would be the stress tensor at that point. Since stress is defined at a continuum point, we determine the stress tensor as a volume average over a block of material,

$$\sigma_{mk} = 1/N^* \sum_i^{N^*} \beta_{mk}^i, \quad (3)$$

in which the stress tensor is averaged over the total number of atoms  $N^*$ , in the block of material.

## 3. COMPUTATIONAL PROCEDURE

The basic computational cell is shown in Figure 1. The dimensions of this cell are approximately 70x35x12 Å. The cell is periodic in the z-direction and has free surfaces in the y-direction. Four cases are considered for the x-direction boundary condition. These cases are presented in detail in Figure 2. Note that for the cases that have grain boundaries present, the periodic cell consists of two basic cells, one of each grain. Two cases are considered for the y-surfaces. In the first case the surface atoms are fixed in the y- and z-directions, yielding a rigid surface. This case represents the limit of embedding the atomistic crystals in a rigid matrix. For the second case the surface atoms are allowed to move freely in the y- and z-directions. This case represents the limit of embedding the atomistic crystals in a soft matrix.

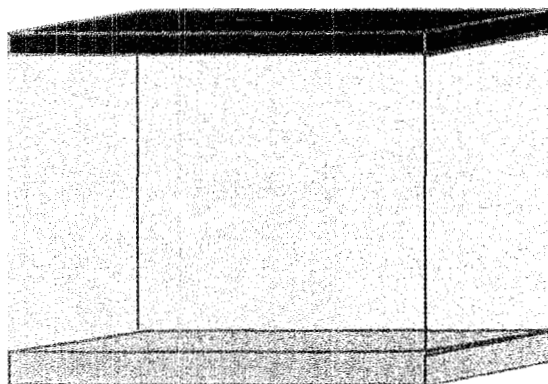
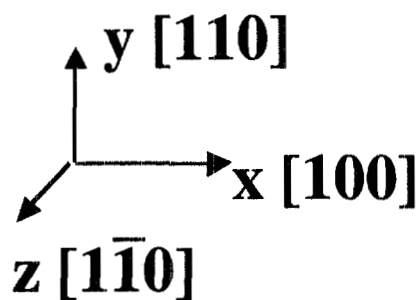


**FIGURE 1.** Geometry for the atomistic calculations. Atoms at the bottom of the computational cell are held fixed. Atoms at the top are moved at constant velocity in x leading to a strain rate of  $10^9$  /s, and the atoms in the center are allowed to move freely with temperature control.

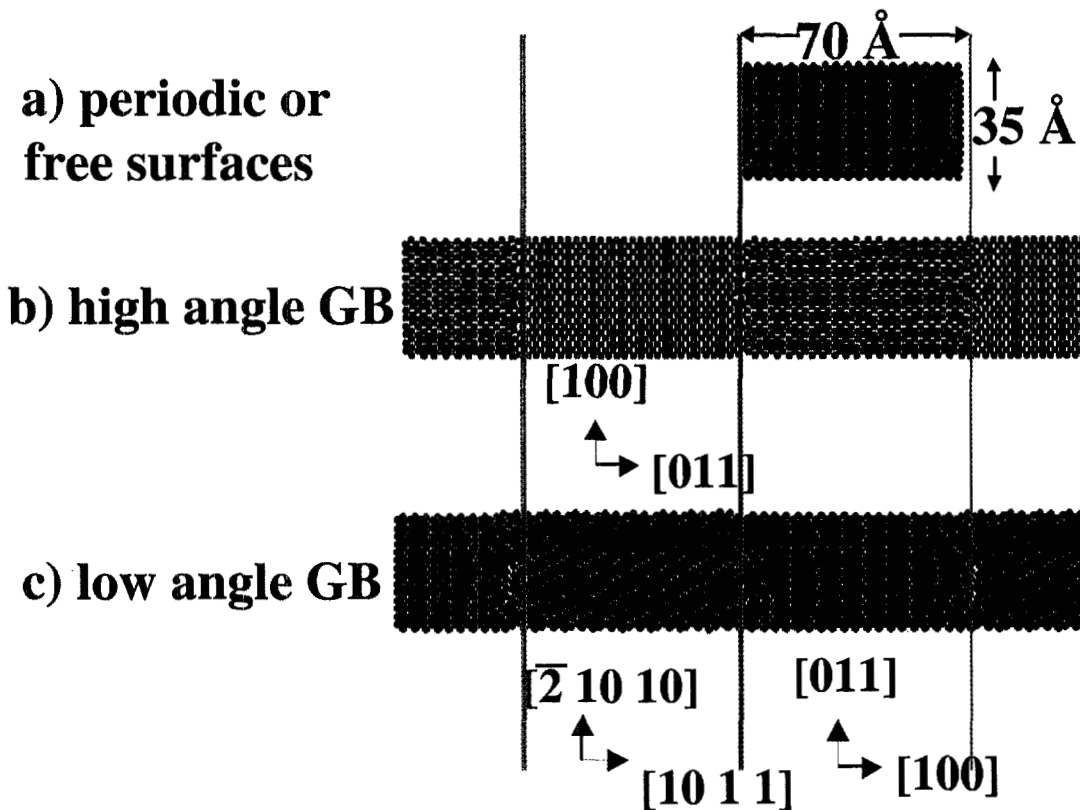


**FIGURE 2.** Geometry for the atomistic calculations. The unit cell has a) periodic or free boundaries representing a single crystal slab or wire respectively. A series of b) high or c) low angle grain boundaries are created by a  $90^\circ$  or  $8^\circ$  rotation around the z-axis of the cell respectively and periodic repetition in the x-direction of the double cell. The vertical lines locate the cell or grain boundaries.

The EAM potentials used are those for Ni taken directly from Angelo et al. [14]. These potentials are known to represent the mechanical properties of Ni quite well.

Standard molecular dynamics techniques with a time step of 1 fs were used. A Nose-Hoover[15] thermostat was used to control the temperature at 300 K. The stress was averaged over the entire computational cell for the total stress calculations and over 15 Å regions in the x-direction to obtain local stresses.

#### 4. RESULTS AND DISCUSSION

The stress-strain curves that result from these calculations are shown in Figure 3. Here we average the stress over the whole cell and normalize it by the shear modulus of the cell. In all cases the stress rises in an approximately linear fashion, representing elastic deformation. We first consider the case of rigid deformation at the y-surfaces (Figure 3a). For three of the four cases, those that include grain boundaries or a free surface in the x-direction, a clear yield point is observed at about 9% strain. The large strain at yield has been discussed previously and is due mainly to crystal size effects[7-12]. For the case of the single crystal slab there is no yield up to 10% strain where the calculations were terminated. Thus we conclude that samples with free surfaces or grain boundaries have lower yield strength than pristine single crystals. What is somewhat surprising is that the yield stress is approximately the same for the wire, the high angle grain boundary, and the low angle grain boundary. We next consider the case of flexible y-surfaces (Figure 3b). The results for the single crystal plate are almost identical to the case for a rigid y-surface. There is clearly no yielding. However, the results for the grain boundary cases are significantly different from the rigid boundary case. We now see yield at a strain about half of what was seen in the rigid boundary case. Relaxing the constraint on the grains allowed yield to occur at a much lower shear strain.

We can start to understand what causes the yield point by examining the atomic displacements. For the case of the rigid y-surface, the atomic displacements at 10% strain relative to the initial atom positions are shown in Figure 4. Here we can see in Figure 4a that for the single crystal slab the deformation is homogeneous. For the other three cases the deformation is clearly inhomogeneous. By examining the displacements after yield it is found that the inhomogeneous behavior is initiated at the free surface or grain boundaries. In fact more detailed analysis of the displacements shows the cause of the inhomogeneous deformation is nucleation of dislocations at the free surface for the case of the wire and at both the high and low angle grain boundaries, i.e., after yield (the large drop in stress) the deformation is inhomogeneous and dislocations are present.

For the case of the flexible y-boundaries, we again see homogeneous deformation for the case of the single crystal plate (Figure 5a). In contrast for the simulations that include grain boundaries (Figure 5bc) we see inhomogeneous deformation that originates from the grain boundaries. Note also that in contrast to the rigid boundary case (Figure 4), the dislocations now are able to exit the y-surfaces rather than be reflected by them. We also can detect a significant rotation of the grains in the high angle case (Figure 5b).

The nucleation of dislocations at grain boundaries and free surfaces has been noted in the literature[1, 2]. It is gratifying that the same mechanism is found to be the controlling factor for yield in the atomistic calculations presented here.

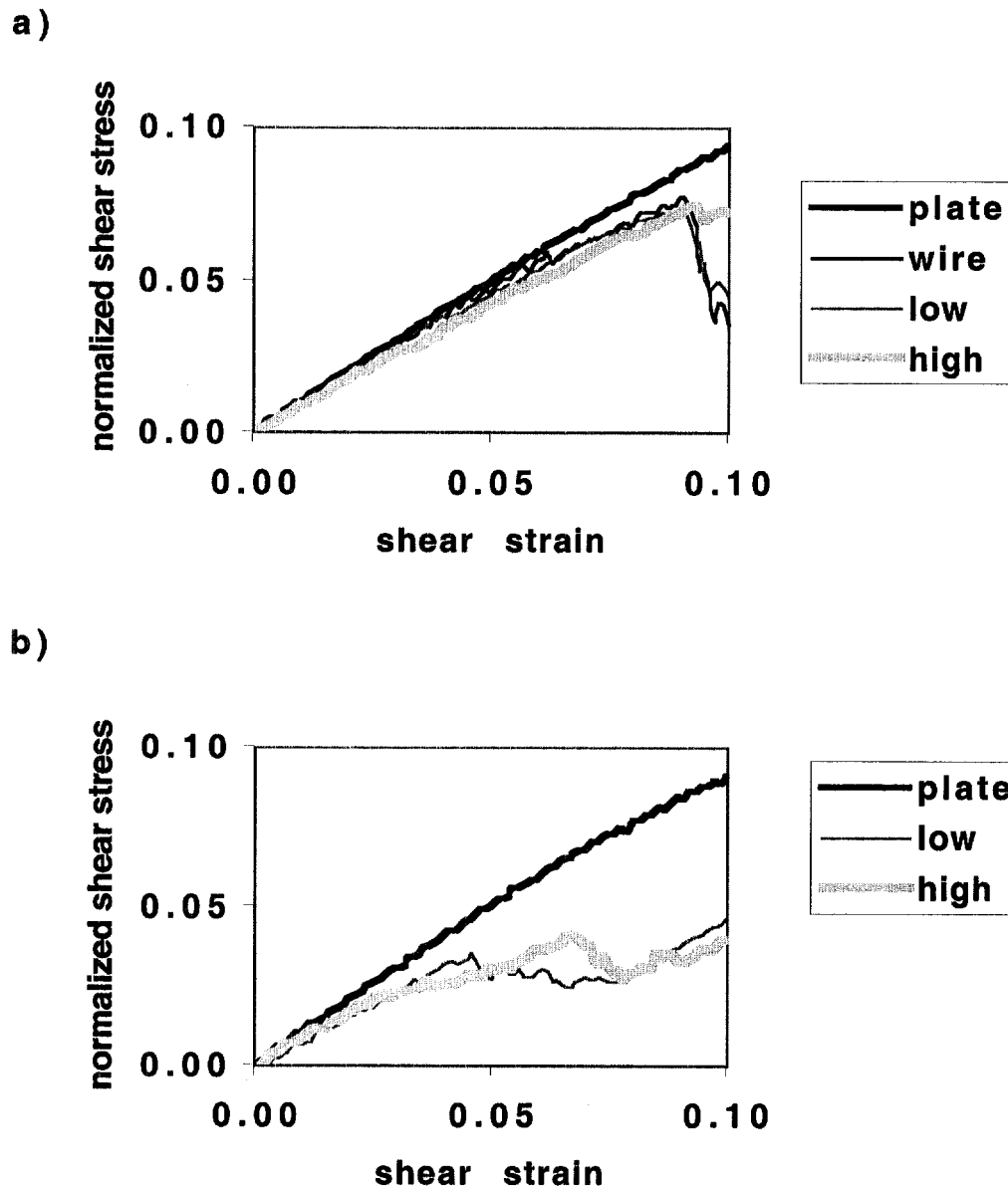


**FIGURE 3.** Stress-strain curves for the four cases considered single crystal plate, single crystal wire, low angle grain boundary, and high angle grain boundary. Boundary condition for y-surface is a) rigid and b) flexible.

We can also investigate the stress in the grain boundary region. Since the calculations represent an array of bi-crystals (*..ABABAB..*), there are two mirror image grain boundaries (AB and BA). Because we shear in a particular direction the response of the two grain boundaries is different. We will call the left grain in Figure 2 grain A and the right grain, grain B. In Figure 6 the local stress at grain boundary AB and BA are compared to the total stress presented previously in Figure 3. For the high angle case the response of grain AB follows the average curve until a stress of just over 2 GPa is obtained. At this stress a clear yield point is observed. Grain BA behaves quite differently. It appears to yield at  $\sim 0.5$  GPa and then again at  $\sim 1$  GPa. It is quite likely that this grain boundary began in a metastable state

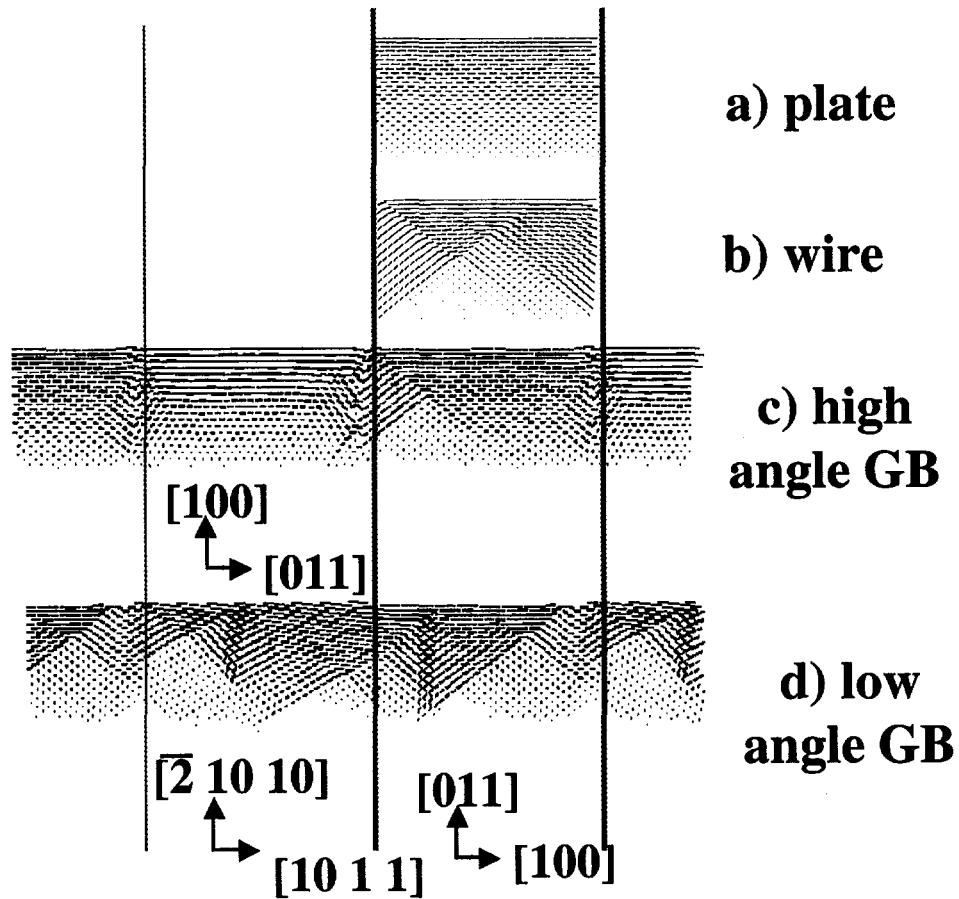


**FIGURE 4.** Atomic displacements at 10% strain for the four cases considered a) single crystal plate, b) single crystal wire, c) high angle grain boundary, and d) low angle grain boundary. The displacements presented are for the case of rigid y-surfaces. The vertical lines locate the cell or grain boundaries.

and the applied shear stress allowed it to relax to a more stable configuration. In any case both grain boundaries yielded at a much lower stress than the apparent average material yield stress. For the low angle grain boundary case, boundary AB appears to be a bit stronger than the average material, but yields at about the same stress. In contrast grain boundary BA has a yield stress about one quarter of the apparent average yield stress. These results show that the macroscopic yield stress of a polycrystalline material does not necessarily represent what is occurring locally

## 5. SUMMARY

We have investigated the behavior of small nickel single crystal and bi-crystal periodic microstructures using the EAM. It is found that in the calculations that have free surfaces or grain boundaries, the deformation is intrinsically inhomogeneous due to dislocation nucleation and propagation. This dislocation nucleation has been directly linked to the existence of a yield point. These results are in complete agreement with experimental observations[1, 2].

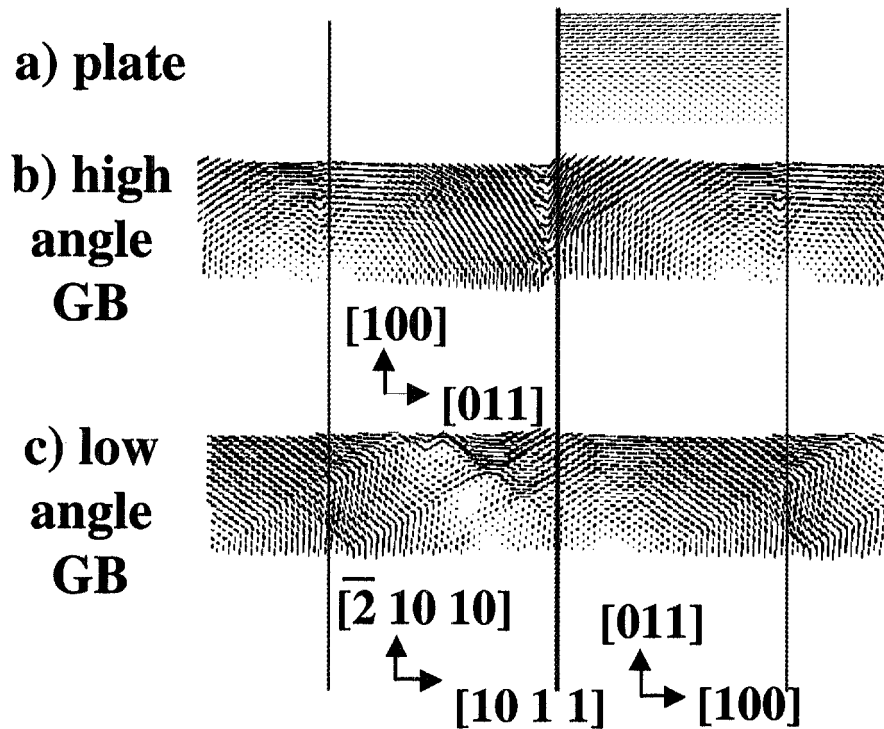


**FIGURE 5.** Atomic displacements at 10% strain for the three cases considered a) single crystal plate, b) high angle grain boundary, and c) low angle grain boundary. The displacements presented are for the case of flexible  $\gamma$ -surfaces. The vertical lines locate the cell or grain boundaries.

### ACKNOWLEDGEMENTS

This work was supported by the US Department of Energy, Office of Science, Office of Basic Energy Sciences, Division of Materials Sciences.

### REFERENCES

- [1] Mitchell, J. W., *phys. stat. sol. (a)* **135**, 455-466 (1993).
- [2] Li, J. C. M., Imam, M. A., Rath, B. B., *J. Materials Science Letters* **11**, 906-908 (1992).
- [3] Daw, M. S., Baskes, M. I., *Phys. Rev. B* **29**, 6443-53 (1984).
- [4] Friedel, J., *Phil Mag* **43**, 153 (1952).
- [5] Stott, M. J., Zaremba, E., *Phys. Rev. B* **22**, 1564 (1980).
- [6] Daw, M. S., Foiles, S. M., Baskes, M. I., *Mater. Sci. Rep.* **9**, 251-310 (1993).
- [7] Horstemeyer, M. F., Baskes, M. I., *J. Engr. Mater. and Tech.* **121**, 114-119 (1999).
- [8] Horstemeyer, M. F., Baskes, M. I., Molecular Dynamics parametric Study of Yield of Single Crystal Nickel, A. S. Khan, Ed., *Plasticity '99: Constitutive and Damage Modeling of Inelastic Deformation and Phase Transformation* (Neat Press, 1999).
- [9] Horstemeyer, M. F., Baskes, M. I., Plimpton, S. J., *Acta Mater.* **49**, 4363-74 (2001).
- [10] Horstemeyer, M. F., Baskes, M. I., Plimpton, S. J., *Theor. and Appl. Fracture Mech.* **37**, 49-98 (2001).
- [11] Horstemeyer, M. F., Baskes, M. I., Godfrey, A., Hughes, D. A., *Int. J. Plasticity* **13**, 203-29 (2001).
- [12] Horstemeyer, M. F., et al., *J. Engr. Mater. Tech.- Trans. ASME* **124**, 322-28 (2002).
- [13] Daw, M. S., Baskes, M. I., *Phys. Rev. Lett.* **50**, 1285-1288 (1983).
- [14] Angelo, J. E., Moody, N. R., Baskes, M. I., *Modelling Simul. Mater. Sci. Eng.* **3**, 289-307 (1995).
- [15] Nose, S., *Prog. Theor. Phys. Suppl.* **103**, 1 (1991).



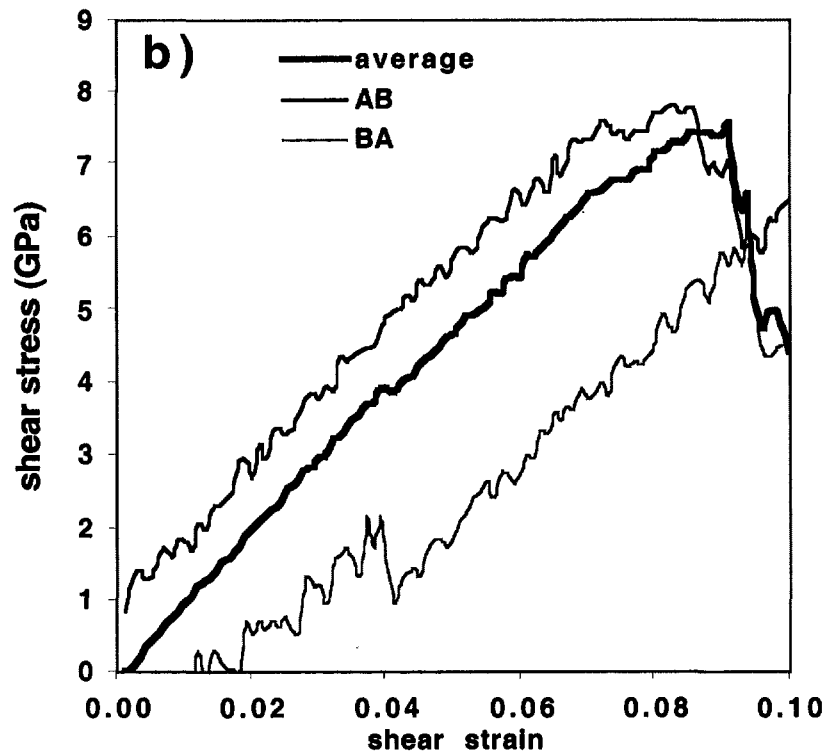
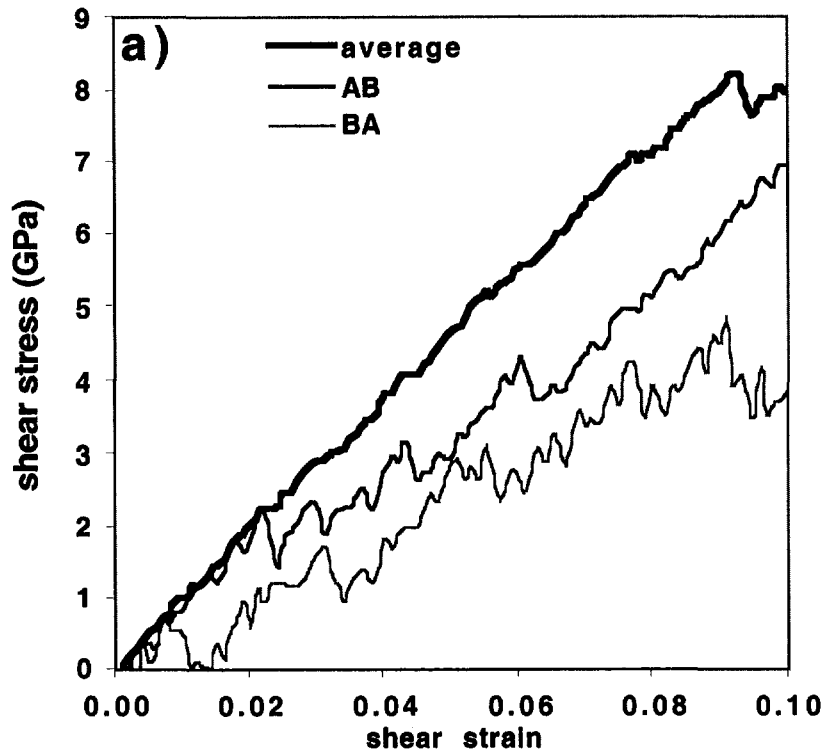


**FIGURE 6.** Average and local shear stress as a function of shear strain for a) the high angle grain boundary case and b) the low angle grain boundary case. The two grain boundaries present in each case are termed AB and BA. Note that in both cases yield appears to occur at the grain boundary before it is detected in the average stress.